Model-assisted extended state observer-based computed torque control for trajectory tracking of uncertain robotic manipulator systems

Chao Chen[1,2,3], Chengrui Zhang[1,2,3] 🄿, Tianliang Hu[1,2,3],
Hepeng Ni[1,2,3] and WeiChao Luo[1,2,3]

Abstract

Computed torque control is an effective control scheme for trajectory tracking of robotic manipulators. However, computed torque control requires precise dynamic models of robotic manipulators and is severely affected by uncertain dynamics. Thus, a new scheme that combines a computed torque control and a novel model-assisted extended state observer is developed for the robust tracking control of robotic manipulators subject to structured and unstructured uncertainties to overcome the disadvantages of computed torque control and exploit its merits. The model-assisted extended state observer is designed to estimate and compensate these uncertain dynamics as a lumped disturbance online, which further improves the disturbance rejection property of a robotic system. Global uniform ultimate boundedness stability with an exponential convergence of a closed-loop system is verified through Lyapunov method. Simulations are performed on a two degree-of-freedom manipulator to verify the effectiveness and superiority of the proposed controller.

Keywords

Robotic manipulator, structured and unstructured uncertainties, computed torque control, extended state observer, trajectory tracking

Introduction

Robotic manipulators are multivariable, time-varying, highly coupled, multi-input multi-output systems that are widely used in industrial automation. Computed torque control (CTC)[1] is a well-known and effective strategy in trajectory tracking control of robotic manipulators among numerous control schemes. A CTC can realize the decoupling control of robotic dynamics and achieve a favorable performance in a trajectory tracking task on the basis of feedback linearization. However, a conventional CTC only works well on the assumption that a precise and complete

[1] School of Mechanical Engineering, Shandong University, Jinan, People's Republic of China
[2] Key Laboratory of High Efficiency and Clean Mechanical Manufacture, Shandong University, Ministry of Education, Jinan, People's Republic of China
[3] National Demonstration Center for Experimental Mechanical Engineering Education, Shandong University, Jinan, People's Republic of China

Corresponding author:
Chengrui Zhang, School of Mechanical Engineering, Shandong University, 17923 Jingshi Road, Jinan 250061, People's Republic of China.
Email: sduzcr@126.com

dynamic model of a manipulator, which is impractical, given the presence of structured and unstructured uncertainties, is available. Structured uncertainties indicate that the dynamic model of a manipulator is clear, but its parameters are inaccurate. Unstructured uncertainties are unmodeled dynamics, including gear frictional forces, external disturbance, high-frequency dynamic modes of a robotic manipulator, and joint and link flexibility. These uncertainties may severely affect the performance of a CTC. Therefore, control of robotic manipulators that are subject to uncertainties has a pivotal role in the field of robotics.[2,3]

Considerable works on modified CTC schemes for uncertain robotic manipulators have been reported to utilize the attractive features of a CTC and alleviate the effects of these uncertainties. Adaptive approaches[4,5] have been introduced to adapt to the varying environment and improve the tracking precision of a manipulator in the presence of structured uncertainties. Wang[6] proposed two adaptive control schemes to realize the objective of task–space trajectory tracking, regardless of uncertain kinematics and dynamics. However, adaptive control law cannot handle unstructured uncertainties. Shi et al.[7] proposed a simple controller with computed torque-like structure enhanced by integral sliding mode, which is posed as a perturbation estimator. Their research indicated that a sliding mode estimator is effective in addressing structured and unstructured uncertainties. However, this estimator causes undesirable chattering, which can degrade the performance of trajectory tracking.

Several intelligent control strategies have been incorporated to alleviate these uncertainties. Neural network is a modern intelligent tool that has been extensively investigated in controlling robotic manipulators considering their universal function approximation and learning capabilities. Gao et al.[8] employed a radial basis function network to approximate the nonlinear uncertainties that degraded the performance of a CTC simultaneously. Doan et al.[9] proposed a new adaptive synchronized CTC algorithm on the basis of neural networks for three degree-of-freedom planar parallel manipulators. The uncertainties of the control system are adaptively compensated online by a bank of neural networks and error compensators. However, the structures of such neural networks are typically complicated, thereby causing heavy computational burden and difficulties in designing and parameter tuning.

A fuzzy logic system is a universal approximator that can be used to learn lumped uncertainties of robotic systems. Song et al.[10] developed a new approach that combines CTC and fuzzy control (FC) for trajectory problems of uncertain robotic manipulator systems. FC, as a compensator, is used to provide auxiliary joint torques to attenuate the influences of uncertainties. Mohan and Bhanot[11] investigated three kinds of conventional CTC plus adaptive control schemes and conducted a comparative study of their performance. Chen et al.[12] incorporated different fuzzy compensators into a CTC for a robust tracking control of a manipulator and compared their performance under the same structured and unstructured uncertainties. Chen et al.[13] proposed a computed-torque plus robust adaptive compensation control scheme using an adaptive FC algorithm and a robust H_∞ control mode to address structured and unstructured uncertainties, respectively. All the aforementioned fuzzy compensators can improve control performance appreciably. However, most of their fuzzy rules are formulated through designers' experience, which is not constantly useful for different circumstances. Furthermore, a lookup table-based controller may be afflicted with the tedious and cumbersome progress of establishing the lookup table.

Observers have also been utilized to tackle uncertainties.[14] In recent years, a novel observer for compensating uncertainties called extended state observer (ESO) has developed rapidly. Han[15] proposed an ESO to estimate the total disturbance in real time. As a summary of all uncertainties in a system, the total disturbance is estimated as an extended state and compensated in a feedforward way. Wang and Gao[16] compared ESO with two other advanced state observers, that is, high-gain and sliding mode, and concluded that ESO is much superior in handling uncertainties and disturbances. ESO-based control schemes have been widely used in industrial control fields,[17–20] including robots.[21–24] However, considerable parameters of a nonlinear ESO that is originally presented by Han is difficult to tune. Moreover, Gao[25] proposed a linear ESO. Linear ESO is essentially a special case of the classic nonlinear ESO. It is convenient to design and has only one tunable parameter that concerns the bandwidth of the observer. Therefore, this ESO is practical.

Nearly all aforementioned applications of ESO in a robotic manipulator control assumed that all of the system knowledge are totally unknown. However, estimating the uncertainties caused by absent model information in complex systems, such as robotic manipulators, is a heavy burden for ESO. Large gains are required to obtain high estimate speed and accuracy, thereby making ESO more sensible to measure noise. If partial knowledge of a robotic system is available, then it can be incorporated into the ESO. Thus, only part of the uncertain model and external disturbances must be estimated. Therefore, the burden of the ESO can be significantly reduced, and the estimation performance can be enhanced.

In this study, a control scheme that combines the conventional CTC and a model-assisted extended state observer (MESO) is proposed for the trajectory tracking control of robotic manipulator systems with structured and unstructured uncertainties. The system can be viewed as two subsystems, namely, a nominal system with a priori knowledge of dynamic model and an uncertain system with all uncertainties and disturbances. The CTC is utilized to handle the nominal system, and the MESO, which serves as a compensator, is used to estimate and eliminate structured and unstructured uncertainties as a lumped disturbance online. The approach fully uses known dynamic knowledge and is convenient to implement. The Lyapunov stability of the

proposed controller is analyzed, and the global uniform ultimate boundedness (GUUB) of a closed-loop system with exponential convergence is proved. The effectiveness and priority of the proposed algorithm are demonstrated by simulations on a two-link planar robotic manipulator.

The remainder of this article is organized as follows. The "Problem formulation" section presents the robotic dynamics and formulates the problem. The "Design of the MESO compensator" section designs the MESO for compensating uncertain dynamics. The "Stability Analysis" section discusses the CTC-MESO controller and verifies the stability through Lyapunov stability theory. The "Simulation results" section illustrates the feasibility and performance of the proposed controller through simulations. Finally, the "Conclusion" section summarizes the conclusions drawn from this study.

Problem formulation

According to Lagrangian or Newton–Euler formulation, the dynamical equation of an *n*-link rigid robotic manipulator with uncertainties can be presented as

$$M(q)\ddot{q} + C(q,\dot{q})\dot{q} + G(q) + F_r(\dot{q}) = \tau + \tau_d \quad (1)$$

where $q, \dot{q}, \ddot{q} \in R^n$ are the vectors of generalized joint angular positions, velocities, and accelerations, correspondingly. $M(q) \in R^{n \times n}$ is a symmetric positive definite inertia matrix; $C(q,\dot{q})\dot{q} \in R^n$ denotes the centrifugal and Coriolis forces, $G(q) \in R^n$ represents the gravity vectors, $F_r(\dot{q}) \in R^n$ expresses the friction forces, $\tau \in R^n$ represents the joint drive torques, and $\tau_d \in R^n$ denotes external disturbances.

In this study, the following assumptions are required.

Assumption 1. The desired trajectory $q_d \in R^n$ belongs to C^2 and bounded.

Assumption 2. The joint angular position q and velocity $\dot{q}$ are measurable as feedback vectors.

If $F_r(\dot{q})$ and τ_d are neglected, then an exact dynamic knowledge of a manipulator can be obtained, and the conventional CTC can be written as

$$\tau = M(q)(\ddot{q}_d - k_v\dot{e} - k_pe) + C(q,\dot{q})\dot{q} + G(q) \quad (2)$$

where $e = q - q_d$; $\dot{e} = \dot{q} - \dot{q}_d$ represent the trajectory tracking errors; and $q_d, \dot{q}_d, \ddot{q}_d \in R^n$ are the vectors of the desired joint angular positions, velocities, and accelerations, respectively. $k_v, k_p \in R^{n \times n}$ are the derivative and proportional gain matrices, which are diagonal positive definite, correspondingly.

The substitution of equation (2) into equation (1) results in a closed-loop system equation as

$$\ddot{e} + k_v\dot{e} + k_pe = 0 \quad (3)$$

If k_v and k_p are selected properly, then the errors will be zero asymptotically.

However, achieving the exact dynamic models of the manipulators is infeasible, and the unmodeled dynamics cannot be ignored in practice. The nominal model is denoted by $M_0(q), C_0(q,\dot{q})$, and $G_0(q)$, and the following relationships can be obtained

$$\begin{aligned} M(q) &= M_0(q) - \Delta M(q) \\ C(q,\dot{q}) &= C_0(q,\dot{q}) - \Delta C(q,\dot{q}) \\ G(q) &= G_0(q) - \Delta G(q) \end{aligned} \quad (4)$$

where $\Delta M(q), \Delta C(q,\dot{q})$, and $\Delta G(q)$ are the uncertain parts. If the precise dynamic models of robotic manipulators are unknown, then equation (2) can be rewritten as

$$\tau = M_0(q)(\ddot{q}_d - k_v\dot{e} - k_pe) + C_0(q,\dot{q})\dot{q} + G_0(q) \quad (5)$$

The substitution of equation (5) into equation (1) yields

$$\ddot{e} + k_v\dot{e} + k_pe = f \quad (6)$$

where

$$f = M_0^{-1}(q)\left(\Delta M(q)\ddot{q} + \Delta C(q,\dot{q})\dot{q} + \Delta G(q) - F_r(\dot{q}) + \tau_d\right). \quad (7)$$

Here, f aggregates the structured and unstructured uncertainties. Moreover, the presence of f can deteriorate the tracking performance of the conventional CTC and may render the robot system unstable.

To improve robustness, a compensator is designed to eliminate the effects of uncertainties caused by friction, parameter variation, external disturbance, and load variation. The new control law of a CTC plus a compensator can be expressed as

$$\begin{aligned} \tau &= \tau_0 + \tau_c \\ \tau_0 &= M_0(q)(\ddot{q}_d - k_v\dot{e} - k_pe) + C_0(q,\dot{q})\dot{q} + G_0(q) \\ \tau_c &= -M_0(q)\hat{f} \end{aligned} \quad (8)$$

where τ_0 is the torque provided by the conventional CTC in equation (5), τ_c expresses the torque produced by the desired compensator, and $\hat{f}$ is the estimated f. The MESO compensator is designed to estimate the function f, given its excellent estimation capability. The configuration of the MESO-based CTC scheme is illustrated in Figure 1.

Design of the MESO compensator

A novel observe algorithm called MESO is utilized to obtain a real-time estimation of uncertainties and disturbances.

The MESO is constructed as follows.

We can deduce that $M_0(q)$ is invertible because it is positive definite symmetric. From equations (1) and (4), the dynamic equation of the robot system can be rewritten as

$$\ddot{q} = M_0^{-1}(q)\tau - M_0^{-1}(q)[C_0(q,\dot{q}) + G_0(q)] + f \quad (9)$$

If $x_1 = q, x_2 = \dot{q}$, then equation (9) can be expressed as
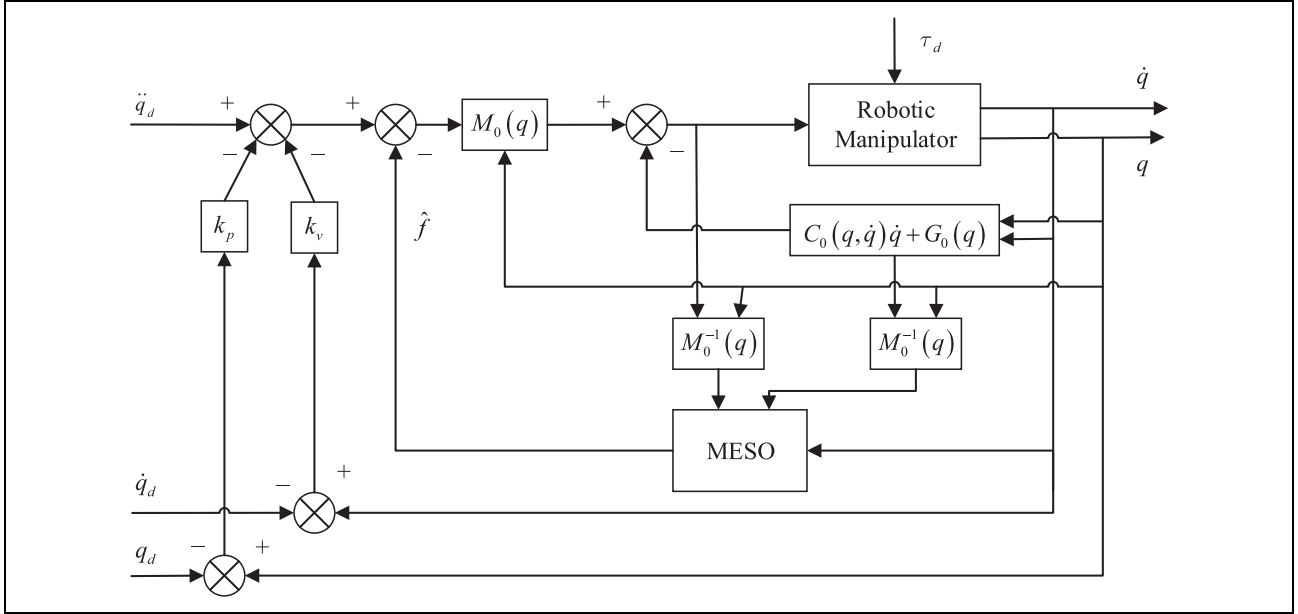
Figure 1. Block diagram of the CTC-MESO control scheme. CTC: computed torque control; MESO: model-assisted extended state observer.

$$\begin{cases} \dot{x}_1 = x_2 \\ \dot{x}_2 = U + H + f \end{cases} \quad (10)$$

where $U = M_0^{-1}(q)\tau \in R^n$ and $H = -M_0^{-1}(q)[C_0(q,\dot{q}) + G_0(q)] \in R^n$. If f is continuous and differentiable in the time domain, then $x_3 = f \in R^n$ is selected as an augmented state. The system (10) can be expanded into

$$\begin{cases} \dot{x}_1 = x_2 \\ \dot{x}_2 = U + H + x_3 \\ \dot{x}_3 = h(t) \end{cases} \quad (11)$$

where $h(t) = \dot{f}$ is an unknown function.

If $x_k = [x_{1k} \cdots x_{nk}]^T$, $k = 1, 2, 3$, $U = [U_1 \cdots U_n]^T$, $H = [H_1 \cdots H_n]^T f = [f_1 \cdots f_n]^T$, and $h(t) = [h_1(t) \cdots h_n(t)]^T$, then the dynamic equation of the ith joint subsystem can be written as

$$\begin{cases} \dot{x}_{i1} = x_{i2} \\ \dot{x}_{i2} = U_i + H_i + x_{i3} \\ \dot{x}_{i3} = h_i(t). \end{cases} \quad (12)$$

where $|h_i|$ is assumed to be bounded. According to assumption 2, joint velocity $\dot{q}$ is measurable. Then, a second-order linear MESO can be designed for i-joint subsystem (12) to estimate f_i for online compensation. The MESO can be constructed as follows:

$$\begin{cases} \dot{\hat{x}}_{i2} = \hat{x}_{i3} + \beta_{i1}(x_{i2} - \hat{x}_{i2}) + U_i + H_i \\ \dot{\hat{x}}_{i3} = \beta_{i2}(x_{i2} - \hat{x}_{i2}) \end{cases} \quad (13)$$

where $\hat{x}_{i2}$ and $\hat{x}_{i3}$ are the estimated x_{i2} and x_{i3}, respectively. β_{i1} and β_{i2} are the observer gains, which can be

determined systematically through the pole placement technique. The characteristic equation of the MESO can be inferred as

$$(s + \omega_{io})^2 = s^2 + 2\omega_{io} + \omega_{io}^2 \quad (14)$$

where ω_{io} is denoted as the bandwidth of the state observer, which is the only tuning parameter. Then, we can derive that

$$\beta_{i1} = 2\omega_{io}, \beta_{i2} = \omega_{io}^2. \quad (15)$$

The estimation error $\tilde{x}_{ij} = x_{ij} - \hat{x}_{ij}$, $j = 2, 3$, is defined. From equations (12), (13), and (15), the estimation error can be presented as

$$\begin{cases} \dot{\tilde{x}}_{i2} = \tilde{x}_{i3} - 2\omega_{io}\tilde{x}_{i2} \\ \dot{\tilde{x}}_{i3} = h - \omega_{io}^2\tilde{x}_{i2} \end{cases} \quad (16)$$

If $\varepsilon_i = [\tilde{x}_{i2} \quad \tilde{x}_{i3}]^T$, $j = 2, 3$, then equation (16) can be rearranged as

$$\dot{\varepsilon}_i = A\varepsilon_i + p(t) \quad (17)$$

where

$$A = \begin{bmatrix} -2\omega_{io} & 1 \\ -\omega_{io}^2 & 0 \end{bmatrix}, p(t) = \begin{bmatrix} 0 \\ h_i(t) \end{bmatrix},$$

Here, A is Hurwitz.

Lemma 1[26]. For any Hurwitz matrix A and $t > 0$, a positive constant C exists. Thus,

$$\|e^{At}\| \leq ce^{\frac{\lambda_{max}(A)}{2}t} \quad (18)$$

where $\lambda_{\max}(A) = \max_{1 \le i \le n}\{\mathrm{Re}\left(\lambda_i(A)\right)\}$, and $\lambda_i(A)$, $i = 1, 2, \ldots, n$ denote the eigenvalues of A.

Lemma 2. The designed MESO for subsystem (12) is considered, and if $h_i(t)$ is bounded, then a constant $\sigma_i > 0$ exists; thus,

$$|\varepsilon_i| \le \sigma_i, i = 1, 2, \ldots, n \qquad (19)$$

That is, the estimation error of the MESO is bounded within a finite time.

Proof. Solving equation (17) follows that

$$\varepsilon_i = e^{(t-t_0)A}\varepsilon_i(t_0) + \int_{t_0}^t e^{(t-\tau)A}p(\tau)\,\mathrm{d}\tau \qquad (20)$$

where t_0 is the initial time. According to lemma 1, we can obtain

$$||e^{(t-t_0)A}|| \le ae^{-\omega_{io}(t-t_0)} \qquad (21)$$

where $a > 0, b > 0$.

Thus, we can obtain

$$\begin{aligned} \varepsilon_i &\le ae^{-\omega_{io}(t-t_0)}||\varepsilon_i(t_0)|| + \int_{t_0}^t ae^{-\omega_{io}(t-t_0)}||p(\tau)||\,\mathrm{d}\tau \\ &\le ae^{-\omega_{io}(t-t_0)}||\varepsilon_i(t_0)|| + \frac{a}{\omega_{io}} \sup_{t_0 \le \tau \le t}||p(\tau)|| \end{aligned} \qquad (22)$$

The first term decreases exponentially. Therefore, the estimation error is bounded by $|\varepsilon_i| \le \sigma_i$ within a finite time, where σ_i is a positive constant whose value is determined by a, ω_{io}, and the upper bound of $||p(\tau)||$. The proof is completed.

We define

$$\hat{f} = \hat{x}_3 \qquad (23)$$

where $\hat{x}_3 = [\hat{x}_{13} \cdots \hat{x}_{n3}]$ is the output of the MESO.

Let $\sigma = [\sigma_1 \ldots \sigma_n]^{\mathrm{T}}$, $\omega_o = [\omega_{1o} \ldots \omega_{no}]^{\mathrm{T}}$, and $\tilde{f}$ be the observer estimation error of f. Lemma 2 indicates that

$$|\tilde{f}| = |f - \hat{f}| \le \sigma \qquad (24)$$

Remark 1. Lemma 2 shows that the estimation error of the MESO is bounded. A large observer gain ω_o indicates a small estimation error. Furthermore, a large gain increases the speed at which the MESO tracks the total disturbance. However, a high gain leads to an increased noise sensitivity. In this study, the dynamic modeling information is incorporated in the MESO, which can reduce the requirement for high observer gains and further enable the MESO to be minimally susceptible to sensor noise.

Remark 2. Lemma 2 is obtained under the assumption that $h(t)$, that is, the rate of change of uncertainty, is bounded. In particular, the performance of the ESO cannot be guaranteed in the presence of fast-varying uncertainties. The generalized or high-order ESO can be used as an effective alternative to address the abovementioned issue. For example, Godbole et al.[27] analyzed a high-order ESO in addressing a fast-varying sinusoidal disturbance. The results showed that a high-order ESO is more precise than the conventional ESO if the gains are well tuned.

Following the aforementioned results, the controller (8) can be implemented at present. The architecture of the overall closed-loop system is depicted in Figure 1.

Stability analysis

Let $k_p = \mathrm{diag}\{k_{1p} \cdots k_{np}\}$, $k_v = \mathrm{diag}\{k_{1v} \cdots k_{nv}\}$, where $k_{ip} > 1$ and $k_{iv} > 0$.

Lemma 3. Let $V(t)$ be the Lyapunov function of any given continuous time system.[28] If $V(t)$ satisfied the following differential inequality, then

$$\dot{V} \le -\lambda V + \phi(t) \qquad (25)$$

where λ is a positive constant, and $\phi(t) > 0$, $\forall t > 0$. If $\phi(t) = C$ is a constant or $\lim_{t \to \infty} \phi(t) = C$, then the closed-loop system can be guaranteed to be the GUUB for any given t_0. In addition, function $V(t)$ satisfies the following inequality

$$V(t) \le \frac{1}{\lambda}[C - \left(C - \lambda V(t_0)\right)\exp(-\lambda t)], \forall t > t_0. \qquad (26)$$

If assumptions 1 and 2 hold, then the following theorem can be stated:

Theorem 1. The robotic manipulator system (1) with uncertainties is considered. If $h(t)$ is bounded, then the control law (8) that combines the CTC and MESO, with equations (13) and (15), can guarantee the GUUB of the closed-loop system.

Proof. Let $k_p = k_1 k_2 + 1$, $k_v = k_1 + k_2$, $k_1 = diag[k_{i1} \cdots k_{n1}]$, and $k_2 = diag[k_{i2} \cdots k_{n2}]$.

We define an error variable

$$z = \dot{e} + k_1 e \qquad (27)$$

The time derivative of z can be inferred as

$$\begin{aligned} \dot{z} &= \ddot{q} - \ddot{q}_d + k_1\dot{e} \\ &= M_0^{-1}(q)\tau + H + f - \ddot{q}_d + k_1\dot{e} \end{aligned} \qquad (28)$$

The Lyapunov function V is defined as follows

$$V = \frac{1}{2}e^2 + \frac{1}{2}z^2 \qquad (29)$$

The derivative of V with respect to time is

$$\begin{aligned} \dot{V} &= e\dot{e} + z\dot{z} \\ &= ez - k_1 e^2 + z\left(M_0^{-1}(q)\tau + H + f - \ddot{q}_d + k_1\dot{e}\right). \end{aligned} \qquad (30)$$
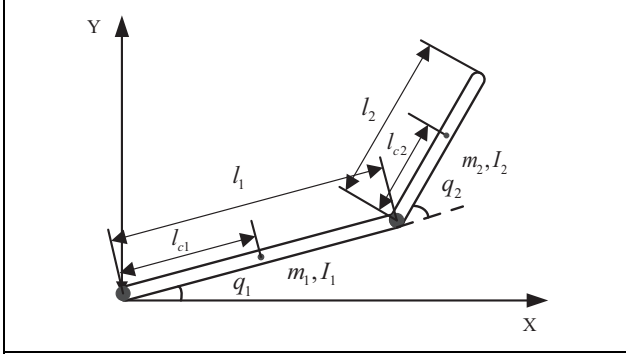
Figure 2. Two-link planar elbow manipulator.

Table 1. Simulation parameters of the two-link robotic manipulator.

Symbol	Definition	Actual value	Nominal value
m_1	Mass of link 1	4 kg	3 kg
m_2	Mass of link 2	2 kg	3 kg
l_1	Length of link 1	0.5 m	0.5 m
l_2	Length of link 2	0.25 m	0.25 m
l_{c1}	Distance to the center of mass of link 1	0.25 m	0.4 m
l_{c2}	Distance to the center of mass of link 2	0.15 m	0.1 m
I_1	Inertia tensor of link 1	1 kg · m^2	0.5 kg · m^2
I_2	Inertia tensor of link 2	0.8 kg · m^2	1 kg · m^2
g	Gravity acceleration	9.8 m/s^2	9.8 m/s^2

The substitution of the control law (8) into equation (30) yields

$$\dot{V} = ez - k_1 e^2 + z\left(-k_2(\dot{e} + k_1 e) - e + \tilde{f}\right)$$

$$= ez - k_1 e^2 + z(-k_2 z - e + \tilde{f})$$

$$= -k_1 e^2 - k_2 z^2 + z\tilde{f}$$

$$\leq -k_1 e^2 - k_2 z^2 + z^2 + \frac{1}{4}\tilde{f}^2 \qquad (31)$$

$$\leq -k_1 e^2 - (k_2 - 1)z^2 + \frac{1}{4}\sigma^2$$

$$\leq -\lambda V + C$$

where $\lambda = \min\{k_1, k_2 - 1\}$ and $C = \sup\limits_{t\to\infty}\left\{\frac{1}{4}\sigma^2\right\}$.

According to lemma 3, the closed-loop system can be guaranteed to be GUUB. The exponential convergence rate of V is specified by λ. If $X = [e, z]^T$, then X is in the compact set $\Omega = \left\{X | \|X\|^2 \leq \frac{2C}{\lambda}\right\}$. In addition, the ultimate bound can be monotonously small by increasing the observer bandwidth ω_o. The exponential convergence rate of V to the bound is specified by λ.

Simulation results. In this section, simulations with a two-link planar elbow manipulator[29] demonstrated in Figure 2 are conducted to verify the efficiency and superiority of the proposed controller. The dynamic equation of the robotic manipulator in equation (1) is derived as follows

$$\begin{bmatrix} m_{11}(q) & m_{12}(q) \\ m_{21}(q) & m_{22}(q) \end{bmatrix}\begin{bmatrix} \ddot{q}_1 \\ \ddot{q}_2 \end{bmatrix} + \begin{bmatrix} c_1(q,\dot{q}) \\ c_2(q,\dot{q}) \end{bmatrix} + \begin{bmatrix} g_1(q) \\ g_2(q) \end{bmatrix} + \begin{bmatrix} f_1(\dot{q}) \\ f_2(\dot{q}) \end{bmatrix}$$

$$= \begin{bmatrix} \tau_1 \\ \tau_2 \end{bmatrix} + \begin{bmatrix} \tau_{d1} \\ \tau_{d2} \end{bmatrix}$$

$$(32)$$

where

$$m_{11}(q) = m_1 l_{c1}^2 + m_2(l_1^2 + l_{c2}^2) + 2m_2 l_1 l_{c2}\cos(q_2) + I_1 + I_2$$
$$m_{12}(q) = m_2 l_{c2}^2 + m_2 l_1 l_{c2}\cos(q_2) + I_2$$
$$m_{21}(q) = m_{12}(q_2)$$
$$m_{22}(q) = m_2 l_{c2}^2 + I_2$$
$$c_1(q,\dot{q}) = -2m_2 l_1 l_{c2}\dot{q}_1\dot{q}_2\sin(q_2) - m_2 l_1 l_{c2}\dot{q}_2^2\sin(q_2)$$
$$c_2(q,\dot{q}) = m_2 l_1 l_{c2}\dot{q}_1^2\sin(q_2)$$
$$g_1(q) = m_1 l_{c1} g\cos(q_1) + m_2 g[l_{c2}\cos(q_1 + q_2) + l_1\cos(q_1)]$$
$$g_2(q) = m_2 l_{c2} g\cos(q_1 + q_2)$$
$$f_1(\dot{q}) = 5.0\dot{q}_1 + 3.0\,\mathrm{sgn}(\dot{q}_1)$$
$$f_2(\dot{q}) = 4.0\dot{q}_2 + 2.0\,\mathrm{sgn}(\dot{q}_2)$$

$$(33)$$

$f_i(\dot{q})$ denotes the viscous and Coulomb frictions of the ith link. The physical parameters of the robotic manipulator used in the simulations are listed in Table 1.

The control objective aims to design a controller to enable the angles of the joints to track desired reference trajectories well while time extends infinitely. The desired joint trajectories are selected as $q_d = [q_{d1}, q_{d2}]^T$ with $q_{d1} = q_{d2} = (1 - e^{-0.05t})\sin(\pi t)$. The initial conditions of the joints are $q_1(0) = 0.5$ rad, $q_2(0) = 0.5$ rad, $\dot{q}_1(0) = 0$ rad/s, and $\dot{q}_2(0) = 0$ rad/s. The sampling period T is selected as 1 ms.
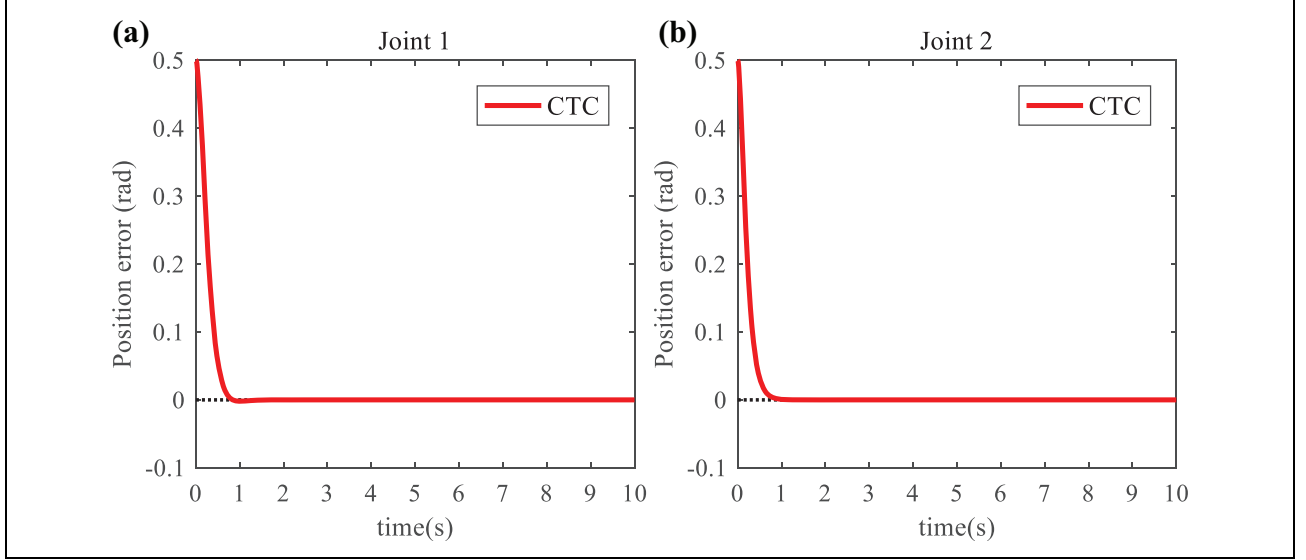
The following performance indices are applied[30] to evaluate the performance of control laws.

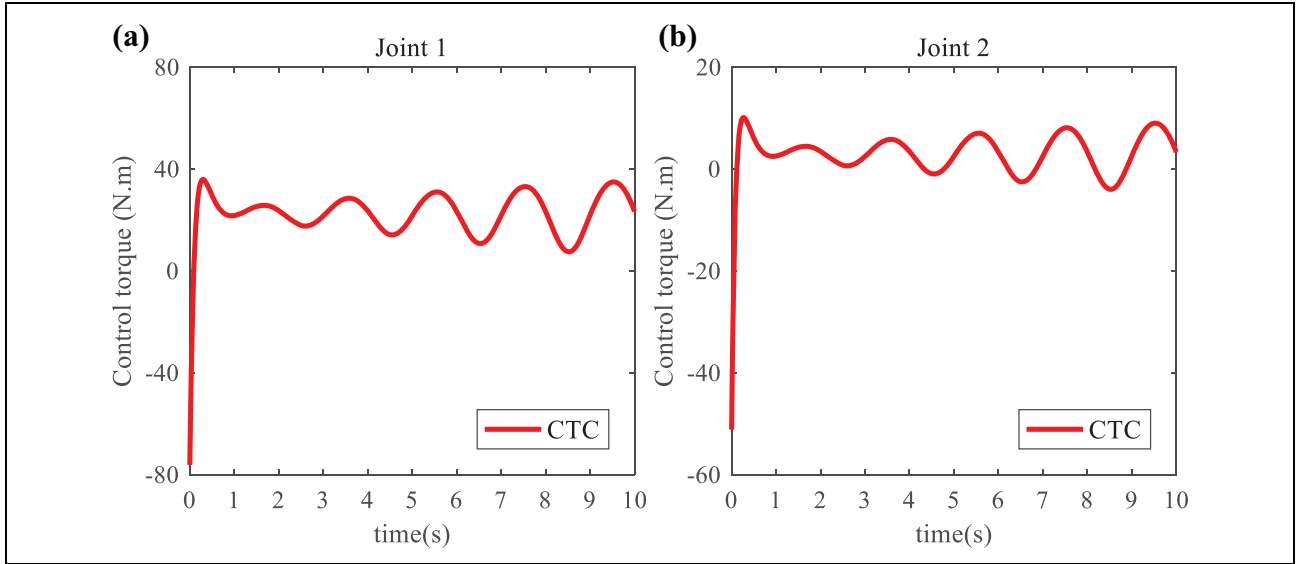A. Integral of the absolute value of the error (IAE)

$$IAE = \int_0^{T_r} |e(t)|\, \mathrm{d}t \qquad (34)$$

B. Integral of the time multiplied by the absolute value of the error (ITAE)

$$ITAE = \int_0^{T_r} t|e(t)|\, \mathrm{d}t \qquad (35)$$

Figure 3. Position tracking error without uncertainties. (a) Joint 1, (b) joint 2. CTC: computed torque control.

Figure 4. Control torque without uncertainties. (a) Joint 1, (b) joint 2. CTC: computed torque control.

IAE and ITAE are error criteria for evaluating the tracking performance of an entire error trajectory, where T_r is the total running time. The IAE penalizes small errors and increases for positive or negative errors. The ITAE criterion penalizes long-duration errors because time appears as a weighting factor in the criterion.

1. *Trajectory tracking without parameter uncertainties or external disturbances*

In this case, the conventional CTC is applied to a robotic system without uncertainties. In particular, a precise dynamical mode is assumed to be obtained. In addition, external disturbances and friction forces are negligible. The control law is obtained as

$$\tau = \tau_0 = M_0(q)(\ddot{q}_d - k_v\dot{e} - k_pe) + C_0(q,\dot{q})\dot{q} + G_0(q) \tag{36}$$

The designed parameters are selected as $k_v = \text{diag}(40, 80)$ and $k_p = \text{diag}(11, 18)$.

Figures 3 and 4 exhibit the position tracking errors and requested control input torques, respectively. The position tracking error converges to zero immediately after a transient given errors in initial configuration. Thus, the conventional CTC with a precise dynamical model is effective and has a favorable position tracking performance for robotic manipulators without uncertainties. However, uncertainties constantly exist in a practical system, thereby rendering the
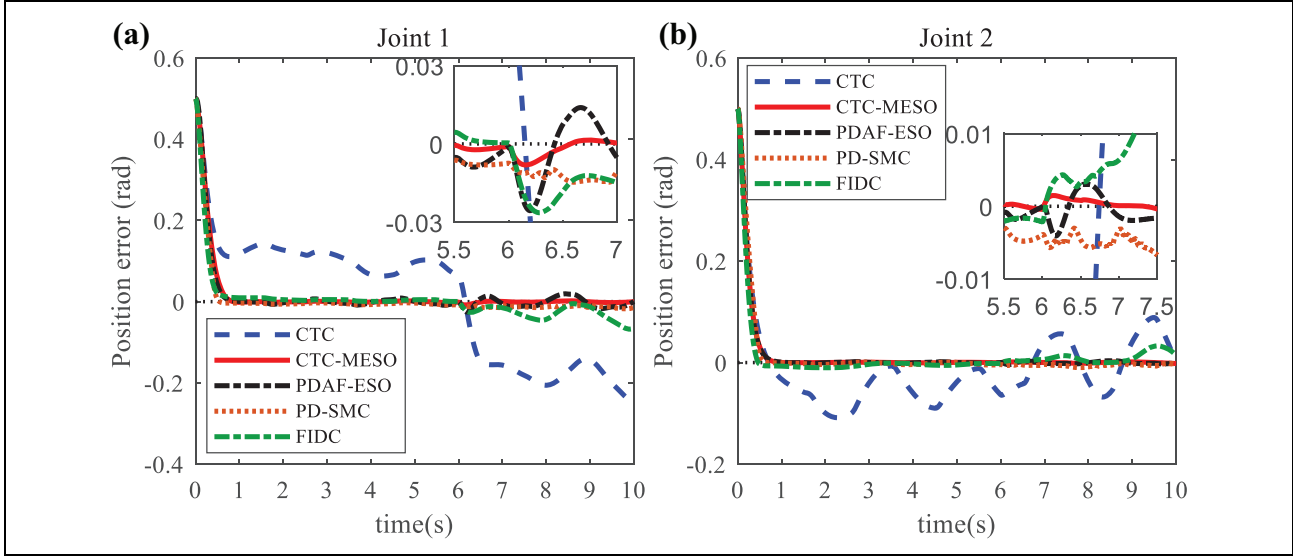
Figure 5. Position tracking error with uncertainties. (a) Joint 1, (b) joint 2. CTC: computed torque control; MESO: model-assisted extended state observer; PD: proportional–derivative; PDAF: PD controller with acceleration feedforward; SMC: sliding mode control; FIDC: finite-time inverse dynamic tracking controller.

conventional CTC minimally attractive when a high performance is required.

2. Trajectory tracking with parameter variations and external disturbances

In this condition, five control laws for the following cases are applied to the robotic manipulator with uncertainties for comparison.

In contrast to a previous case, these controllers are designed using nominal rather than actual parameters, and a friction force is attached to each joint, as expressed in equations (32) and (33). Moreover, external disturbances are considered and assumed to be $\tau_d = [2in(t) + 0.5\sin(200\,\pi t), cos(2t) + 0.5\sin(200\,\pi t)]^{\mathrm{T}}$, where the second terms serve as the effect of high-frequency measurement noises.[31] To test the robustness of the controllers against parameter variations further, the robotic manipulator is assumed to suddenly gather a heavy load. In particular, the mass of link 2 m_2 is increased from 2 kg to 6 kg at $t = 6$ s.

Case 1. The conventional CTC. In this case, the control law is the same as that in equation (36).

Case 2. The proposed CTC-MESO controller. In this case, the control input torque can be obtained by using equation (8).

Case 3. Control without model information. In this case, the control law is the same as that in equation (8), but all model information is assumed to be unknown. Letting $M_0(q) = \mathrm{diag}(1, 1)$, $C_0(q, \dot{q}) = [0; 0]$, $G_0(q) = [0; 0]$, and MESO in equation (13) reduces to

$$\begin{cases} \dot{\hat{x}}_{i2} = \hat{x}_{i3} + \beta_{i1}(x_{i2} - \hat{x}_{i2}) + \tau_i \\ \dot{\hat{x}}_{i3} = \beta_{i2}(x_{i2} - \hat{x}_{i2}) \end{cases} \qquad (37)$$

The control law can be rewritten as

$$\tau = \tau_0 + \tau_c = \ddot{q}_d - k_v\dot{e} - k_p e - \hat{f} \qquad (38)$$

If all model knowledge is discarded, then the CTC-MESO degrades to a proportional–derivative (PD) controller with acceleration feedforward (PDAF) and conventional ESO compensator. The PDAF can be considered a special type of CTC when the model information is absent. Here, total disturbance *f* must be compensated increases to

$$f = \left(I - M(q)\right)\ddot{q} - C(q, \dot{q})\dot{q} - G(q) - F_r(\dot{q}) + \tau_d \quad (39)$$

For comparison, parameters k_v and k_p of all controllers are selected to be the same as those in previous cases. The observer gains are selected as $\omega_0 = [180 \text{ rad/s}, 180 \text{ rad/s}]^{\mathrm{T}}$, and the initial states of MESO and ESO are assumed to be all zeroes.

Case 4. A modified CTC called finite-time inverse dynamic tracking controller (FIDC) proposed by Su and Zheng.[32] The FIDC law is obtained by
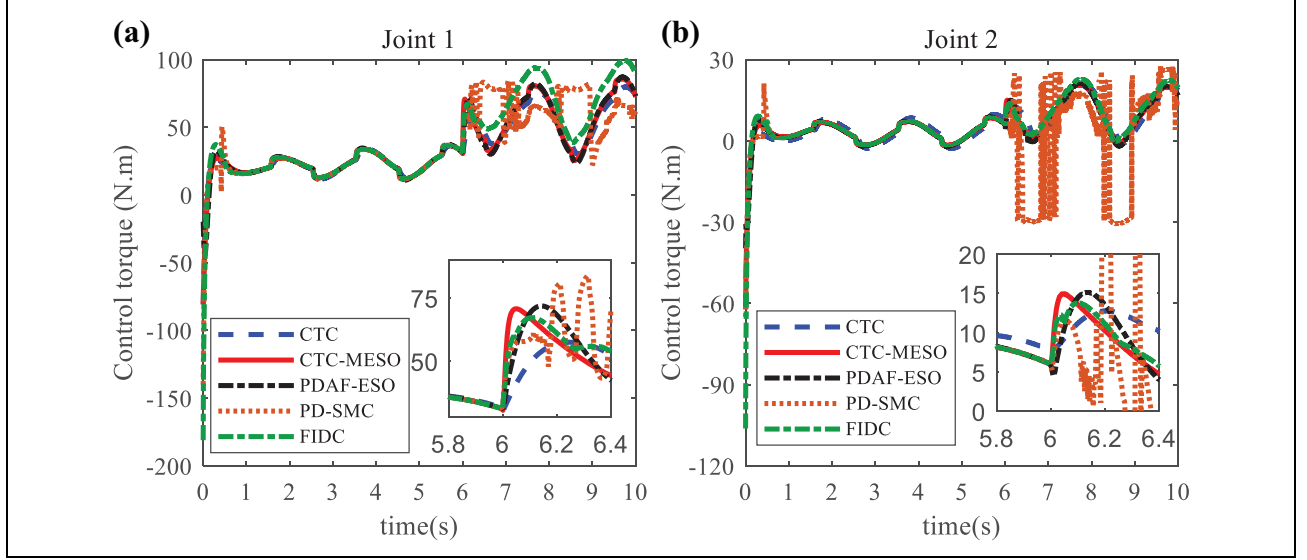
$$\begin{aligned} \tau =\, & M_0(q)[\ddot{q}_d - K_p Sig(e)^{\alpha_1} - K_d Sig(\dot{e})^{\alpha_2}] \\ & + C_0(q, \dot{q})\dot{q} + G_0(q) \end{aligned} \qquad (40)$$

where $K_p = \mathrm{diag}(130, 200)$, $K_d = \mathrm{diag}(40, 80)$, $\alpha_1 = 0.5$, and $\alpha_2 = 2\alpha_1/(\alpha_1 + 1) = 0.667$.

Case 5. A model-free control law called PD with sliding mode control (PD-SMC).[33] The PD-SMC is defined as

$$\tau = K_p e + K_d \dot{e} + H sat(s, \varphi)$$

$$sat(s, \varphi) = \begin{cases} sign(s) \text{ if } |s| > \varphi \\ s/\varphi \quad \text{ if } |s| \le \varphi \end{cases} \qquad (41)$$

Figure 6. Control torque with uncertainties. (a) Joint 1, (b) joint 2. CTC: computed torque control; MESO: model-assisted extended state observer; PD: proportional–derivative; PDAF: PD controller with acceleration feedforward; SMC: sliding mode control; FIDC: finite-time inverse dynamic tracking controller.
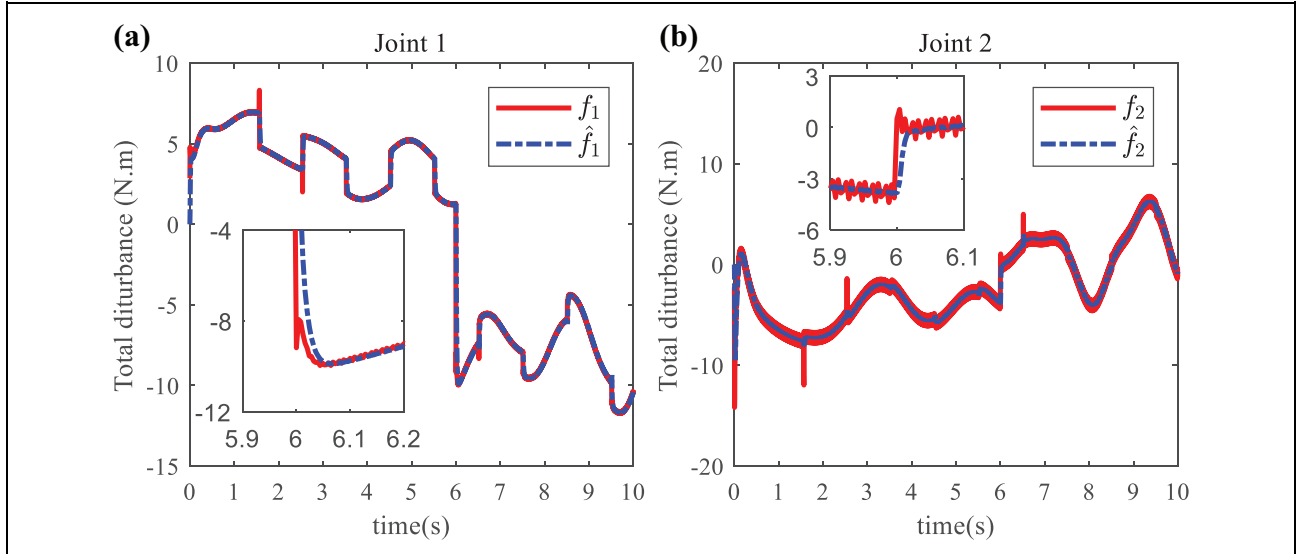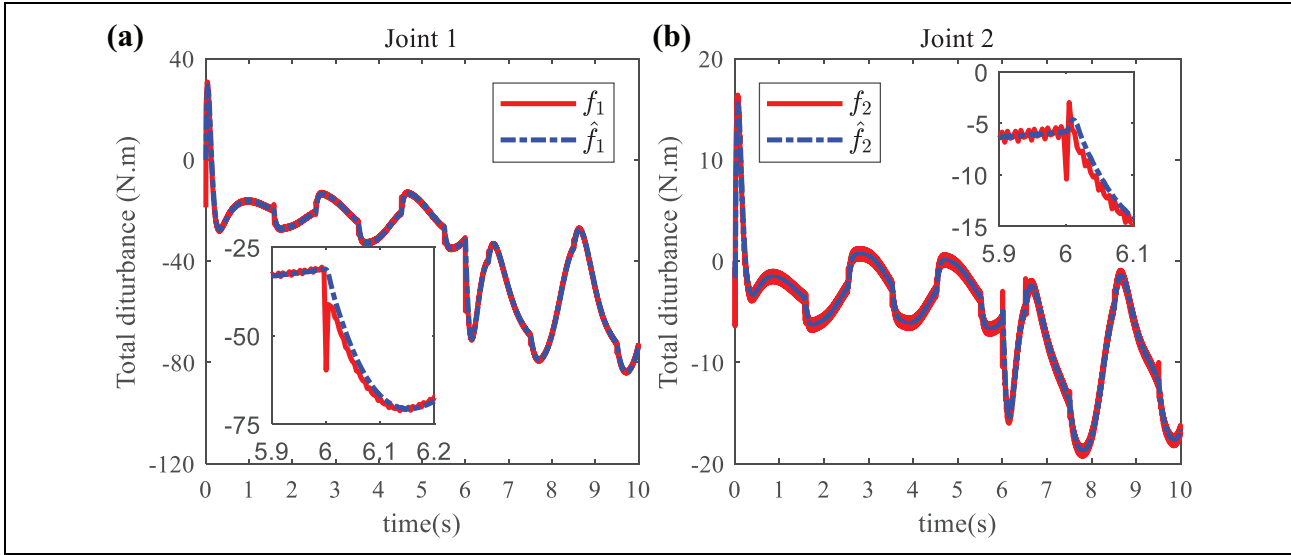

Figure 7. Disturbance estimation of the MESO in case 2. (a) actual total disturbance f_1 of joint 1 subsystem and its estimation $\hat{f}_1$; (b) actual total disturbance f_2 of joint 2 subsystem and its estimation $\hat{f}_2$. MESO: model-assisted extended state observer.

where $e = q_d - q$, $\dot{e} = \dot{q}_d - \dot{q}$, $s = \dot{e} + \lambda e$, $K_p = \text{diag}(150, 80)$, $K_d = \text{diag}(100, 40)$, $H = \text{diag}(65, 25)$, $\lambda = 20$.

Figure 5 depicts the position tracking errors when structured and unstructured uncertainties are considered. Figure 6 displays the corresponding control input torques. Figure 5 demonstrates that the performance of the conventional CTC and FIDC are significantly deteriorated, given parameter variations and external disturbances compared with that in the previous case. The CTC and FIDC cannot handle this severe disturbance well, and the tracking errors display relatively large oscillations, which may cause instability of

the closed-loop control system, when the value of m_2 changes at $t = 6$ s. PD-SMC has high robustness but causes the controlled system chattering, even though a saturation function is employed.

The tracking performance is much better in the CTC-MESO controller than other controllers in the transient and steady states. The tracking errors are remarkably minimal, and unexpected effects can be attenuated well. The system can rapidly return to a stable state with light oscillation when parameter variation occurs. The high-accuracy tracking performance originates from the effectiveness of the

Figure 8. Disturbance estimation of the ESO in case 3. (a) actual total disturbance f_1 of joint 1 subsystem and its estimation $\hat{f}_1$; (b) actual total disturbance f_2 of joint 2 subsystem and its estimation $\hat{f}_2$. ESO: extended state observer.

MESO. Comparison results demonstrate that uncertainties caused by parameter variations and external disturbances can be estimated and compensated by the MESO effectively. Figure 7 illustrates that the estimation error remains minimal, except for the pulse-type error caused by the discontinuity of Coulomb friction when the velocity changes its sign. In particular, the MESO can estimate the total disturbances rapidly and accurately.

Figure 5 depicts that the tracking performance of the PDAF-ESO controller is also remarkably improved over the CTC. However, the oscillations of the tracking errors still cannot be ignored. A fluctuation of position appears when parameter variation occurs suddenly. Figures 7 and 8 exhibit that the time consumed in estimating and compensating for the sudden disturbance is longer in the ESO than in the MESO. In fact, ESO is a special instance of the MESO when model information is unknown. This instance eases the burden on the controller design by requiring minimal model information but at the expense of a high gain to acquire a requirement of a high tracking speed and favorable estimation accuracy of a disturbance in accordance with lemma 2, which results in increased noise sensitivity. Figures 7 and 8 and the comparison between equations (7) and (39) demonstrate that the total disturbances are smaller in case 2 than in case 3. This condition is due to the fact that MESO uses known model information to reduce the estimation burden largely. The MESO must only estimate the total disturbance, which excludes the known partial information. Therefore, the MESO can acquire favorable estimation accuracy and tracking speed without requiring high observer gains, thereby enabling the MESO to be less susceptible to measuring noise than the ESO while still maintaining the simple structure and easiness to implement. The estimation of large uncertainties is a heavy burden for the

Table 2. Performance indices with uncertainties.

Controller	Joint	IAE (rad)	ITAE (rad · s)
CTC	Joint 1	1.3910	7.2045
CTC-MESO	Joint 1	0.0512	0.0944
PDAF-ESO	Joint 1	0.1971	0.4606
PD-SMC	Joint 1	0.1927	0.5253
FIDC	Joint 1	0.2430	1.0215
CTC	Joint 2	0.5863	2.3958
CTC-MESO	Joint 2	0.1169	0.0533
PDAF-ESO	Joint 2	0.1237	0.0939
PD-SMC	Joint 2	0.1519	0.2187
FIDC	Joint 2	0.1583	0.4298

IAE: integral of the absolute value of the error; ITAE: integral of the time multiplied by the absolute value of the error; CTC: computed torque control; MESO: model-assisted extended state observer; PD: proportional–derivative; PDAF: PD controller with acceleration feedforward; SMC: sliding mode control; FIDC: finite-time inverse dynamic tracking controller.

ESO. The ESO fails to offer a satisfactory estimation performance considering the abrupt changes caused by parameter variation or discontinuity of Coulomb friction.

Table 2 and Figure 5 suggest that the tracking performance of the proposed CTC-MESO controller is superior to the conventional CTC and other controllers. The composite controller significantly enhances the quality of control and demonstrates robustness against structured and unstructured uncertainties.

Conclusion

In this study, a modified CTC scheme has been proposed to address the problem of trajectory control of a robot manipulator subjected to structured and unstructured

uncertainties. First, the concept and restrictions of the conventional CTC were reviewed in detail. Second, a MESO compensator was incorporated into the conventional CTC to handle inevitable uncertainties. The MESO was used to estimate the total disturbance, including simultaneous structured and unstructured uncertainties. The stability of the proposed controller was confirmed through Lyapunov theory. Simulations of a two-link elbow planar robot manipulator were conducted to demonstrate the feasibility of the new scheme. The simulations confirmed that the proposed CTC-MESO controller can significantly attenuate the effects of uncertainties and improve the system tracking accuracy and disturbance rejection property in comparison with the conventional CTC and PDAF-ESO. The results indicated that the MESO has higher accuracy and faster response, in the meantime, it provides better disturbance attenuation than the classic ESO. The designed controller has the advantages of simple structure, easy regulation, and solid robustness. Furthermore, the performance improvement is obtained without excessive input control torques, which does not yield the actuator saturation. Therefore, it is suitable for industrial application.

Declaration of conflicting interests

Funding

ORCID iD

Chengrui Zhang https://orcid.org/0000-0003-1536-589X

References

1. Middletone RH and Goodwin GC. Adaptive computed torque control for rigid link manipulators. In: *1986 25th IEEE conference on decision and control*. Athens, Greece, 10–12 December 1986, pp.68–73. Piscataway: IEEE.

2. Mehdi H and Boubaker O. Impedance controller tuned by particle swarm optimization for robotic arms. *Int J Adv Robot Syst* 2011; 8: 57.

3. Mehdi H and Boubaker O. Robust impedance control-based Lyapunov-Hamiltonian approach for constrained robots. *Int J Adv Robot Syst* 2015; 12: 190.

4. Slotine JJ and Weiping L. Adaptive manipulator control: a case study. *IEEE Trans Automat Contr* 1988; 33: 995–1003.

5. Li M, Li Y, Ge SS, et al. Adaptive control of robotic manipulators with unified motion constraints. *IEEE Trans Syst Man Cybern Syst* 2017; 47: 184–194.

6. Wang H. Adaptive control of robot manipulators with uncertain kinematics and dynamics. *IEEE Trans Automat Contr* 2017; 62: 948–954.

7. Shi J, Liu H, and Bajçinca N. Robust control of robotic manipulators based on integral sliding mode. *Int J Contr* 2008; 81: 1537–1548.

8. Gao W, Shi J, Wang W, et al. Research on sliding mode control for robotic manipulator based on RBF neural network. In: *2017 29th Chinese control and decision conference (*CCDC*)*, Chongqing, China, 28–30 May 2017, pp. 4934–4938. Singapore: IEEE Industrial Electronics (IE) Chapter.

9. Doan QV, Le TD, Le QD, et al. A neural network–based synchronized computed torque controller for three degree-of-freedom planar parallel manipulators with uncertainties compensation. *Int J Adv Robot Syst* 2018; 15: 1729881418767307.

10. Song Z, Yi J, Zhao D, et al. A computed torque controller for uncertain robotic manipulator systems: fuzzy approach. *Fuzzy Sets Syst* 2005; 154: 208–226.

11. Mohan S and Bhanot S. Comparative study of some new hybrid fuzzy algorithms for manipulator control. *J Control Sci Eng* 2007; 2007: 303.

12. Chen Y, Bi YJ, and Gao J. Adaptive fuzzy computed-torque control for robot manipulator with uncertain dynamics. *Int J Adv Robot Syst* 2012; 9: 267–270.

13. Chen Y, Ma G, Lin S, et al. Computed-torque plus robust adaptive compensation control for robot manipulator with structured and unstructured uncertainties. *IMA J Math Contr I* 2016; 33: 37–52.

14. Boubaker O and Iriarte R. *The inverted pendulum in control theory and robotics: from theory to new innovations*. Stevenage: IET, 2017.

15. Han J. From PID to active disturbance rejection control. *IEEE Trans Ind Electron* 2009; 56: 900–906.

16. Wang W and Gao Z. A comparison study of advanced state observer design techniques. In: *Proceedings of the 2003 American control conference*, Denver, USA, 4–6 June 2003, pp.4754–4759. Piscataway: IEEE.

17. Li C, Yang H, Jenkins LL, et al. Enhanced-performance control of an electromagnetic solenoid system using a digital controller. *IEEE Trans Contr Syst Technol* 2016; 24: 1805–1811.

18. Zhou X, Zhu J, Zhao B, et al. Extended state observer/proportion integration differentiation compound control based on dynamic modelling for an aerial inertially stabilized platform. *Int J Adv Robot Syst* 2017; 14: 1729881417744354.

19. Wang H, Li S, Lan Q, et al. Continuous terminal sliding mode control with extended state observer for PMSM speed regulation system. *Trans Inst Meas Control* 2017; 39: 1195–1204.

20. Yao J, Jiao Z, and Ma D. Extended-state-observer-based output feedback nonlinear robust control of hydraulic systems with backstepping. *IEEE Trans Ind Electron* 2014; 61: 6285–6293.

21. Wu Y, Du YL, and Zhang W. Decentralized adaptive fuzzy control for manipulator based on extended state observer. *J Southeast Univ* 2012; 42: 192–195.

22. Wu S, Dong B, Ding G, et al. Backstepping sliding mode force/position control for constrained reconfigurable manipulator based on extended state observer. In: *12th world congress on intelligent control and automation (*WCICA*)*, Guilin, China, 12–15 June 2016, pp.477–482. Piscataway: IEEE.

23. Cui R, Chen L, Yang C, et al. Extended state observer-based integral sliding mode control for an underwater robot with unknown disturbances and uncertain nonlinearities. *IEEE Trans Ind Electron* 2017; 64: 6785–6795.

24. Yang H, Yu Y, Yuan Y, et al. Back-stepping control of two-link flexible manipulator based on an extended state observer. *Adv Space Res* 2015; 56: 2312–2322.

25. Gao Z. Scaling and bandwidth-parameterization based controller tuning. In: *Proceedings of the 2003 American control conference*, Denver, USA, 4–6 June 2003, pp.4989–4996. Piscataway: IEEE.

26. Zhang W, Branicky MS, and Phillips SM. Stability of networked control systems. *IEEE Contr Syst* 2001; 21: 84–99.

27. Godbole AA, Kolhe JP, and Talole SE. Performance analysis of generalized extended state observer in tackling sinusoidal disturbances. *IEEE Trans Contr Syst Technol* 2013; 21: 2212–2223.

28. Qu Z, Dawson DM, Dorsey JF, et al. A new class of robust control laws for tracking of robots. In: *Proceedings of the 31st IEEE conference on decision and control*, Tucson, USA, 16–18 December 1992, pp.1408–1409. Piscataway: IEEE.

29. Yang ZJ, Fukushima Y, and Qin P. Decentralized adaptive robust control of robot manipulators using disturbance observers. *IEEE Trans Contr Syst Technol* 2012; 20: 1357–1365.

30. Liu H and Zhang T. Adaptive neural network finite-time control for uncertain robotic manipulators. *J Intell Robot Syst* 2014; 75: 363–377.

31. Yu S, Yu X, Shirinzadeh B, et al. Continuous finite-time control for robotic manipulators with terminal sliding mode. *Automatica* 2005; 41: 1957–1964.

32. Su Y and Zheng C. Global finite-time inverse tracking control of robot manipulators. *Robot Comput Integr Manuf* 2011; 27: 550–557.

33. Ouyang PR, Acob J, and Pano V. PD with sliding mode control for trajectory tracking of robotic system. *Robot Comput Integr Manuf* 2014; 30: 189–200.